

## Novel Precursors of Solvated Electrons in Water: Evidence for a Charge Transfer Process

R. Laenen, T. Roth, and A. Laubereau

*Physik-Department E11, Technische Universität München, D-85748 Garching, Germany*

(Received 21 March 2000)

Femtosecond midinfrared spectroscopy of water (heavy water) after two photon excitation at 9 eV provides clear evidence for two short-lived precursors of the hydrated electron preceding the well-known “wet electron.” The measured first intermediate with peak absorption at 2.9 (4.1)  $\mu\text{m}$  is proposed to represent an  $\text{O}(\text{H}, \text{D}):e^-$  complex. The subsequent solvation proceeds via  $e^-:[(\text{H}, \text{D})_2\text{O}]_n$  complexes at approximately 1.6 (2.0)  $\mu\text{m}$  in the electronic ground state, involving an increasing number of water molecules during the first 200 fs and followed by the wet electron.

PACS numbers: 33.80.Eh, 42.62.Fi

The solvated electron in water has attracted special interest due to the importance of water [1] in physics, chemistry, and biology and the limited understanding of charge transfer processes in condensed matter. The first time-resolved investigations of the ultrafast generation of hydrated electrons were performed several years ago [2–4]. Further experiments have been conducted since then by different groups providing an improved view on the dynamics of the generation process and of the already solvated electron [5–9]. One of the still open questions, which are until now controversially discussed, concerns the nature of the intermediate termed “wet electron,” seen during the formation of the solvated electron. In the literature an assignment of the wet electron to an excited  $2p$  state can be found as well as to a modified (hot) ground state  $1s$  of the electron in its solvation shells. A shortcoming of the previous experiments is the accessible wavelength range of the probing process, commonly restricted to the visible and near IR.

In this contribution we present the first midinfrared observations of the generation of solvated electrons, extending the probing wavelengths to 5.5  $\mu\text{m}$ . Our data shed new light on the dynamics of the charge separation process of water after excitation with 9 eV.

The experiments are conducted with a home-built Ti:sapphire laser system with regenerative amplification of single pulses at 1 kHz repetition rate. The setup supplies UV-pump pulses of 150 fs at 273 nm (4.5 eV) with pulse energy of 8  $\mu\text{J}$  that are focused into a sample jet of thickness  $\approx 75 \mu\text{m}$ . Neat (tridistilled) protonated and deuterated water is investigated. The two photon excitation mechanism was verified experimentally from the measured intensity dependence. The jet is utilized to avoid accumulative thermal effects in the excitation volume. The induced absorption changes of the sample are monitored measuring the energy transmission of weak probing pulses. Tunability of the latter is achieved in a large spectral range from 0.4 up to 5.5  $\mu\text{m}$  using parametric amplification of a white light continuum with subsequent difference frequency mixing. The probe pulse duration depends on the wavelength with values of  $\approx 150$  fs in the visible, decreasing in the near infrared (NIR) to 100 fs at 1.7  $\mu\text{m}$ , and rising for larger wavelengths to  $\approx 300$  fs at

5  $\mu\text{m}$ . Adjusting the polarization plane of the probe at  $45^\circ$  relative to the linearly polarized excitation pulse, the parallel and perpendicular changes of the sample transmission are simultaneously detected in order to measure the induced dichroism [7]. The zero setting of the delay time, which is crucial for the interpretation of the data, is accurately determined for each probing wavelength via two photon absorption in a thin diamond specimen.

Experimental data on the generation process of solvated electrons in  $\text{H}_2\text{O}$  after two photon UV absorption are depicted in Fig. 1 for six probing wavelengths ranging from 1.6 up to 5.5  $\mu\text{m}$ . The parallel component of the transmission change is plotted versus delay time. From the measured transients, one can clearly infer a shift of the maximum induced absorption towards earlier delay times and a more rapid decay with increasing wavelength. We also note that the peak amplitudes depend on the wavelength in a nonmonotonic manner. The induced dichroism of the sample deduced from the measured parallel and perpendicular transmission changes is negligible; an upper limit of 0.005 is set in the whole probing range in the IR by the experimental accuracy.

Corresponding transient probe spectra are presented in Fig. 2. Only part of the data are shown for the wavelength range of 1.4 to 2.35  $\mu\text{m}$  and the delay time interval  $50 \text{ fs} < t_D < 200 \text{ fs}$  (note different line styles and symbols). From the data, a strong shift of the induced absorption is noticed from the midinfrared (MIR) to the NIR within the first 200 fs. In addition, a transient isosbestic point is suggested around 1.85  $\mu\text{m}$  for the time interval 75 fs to 150 fs. The finding presents evidence that the dynamics can be described by an initial species with subsequent relaxation to a further level.

Our data are interpreted with the help of a six-level model which extends earlier approaches to account for novel details of the charge separation process in water. The scheme is depicted in Fig. 3. Via two photon absorption water molecules are promoted from the ground state (level 0) to an electronically excited state (level 1) from which relaxation occurs within our experimental time resolution to a first species (level 2). The latter is characterized by a peak absorption in the MIR and a pronounced isotope

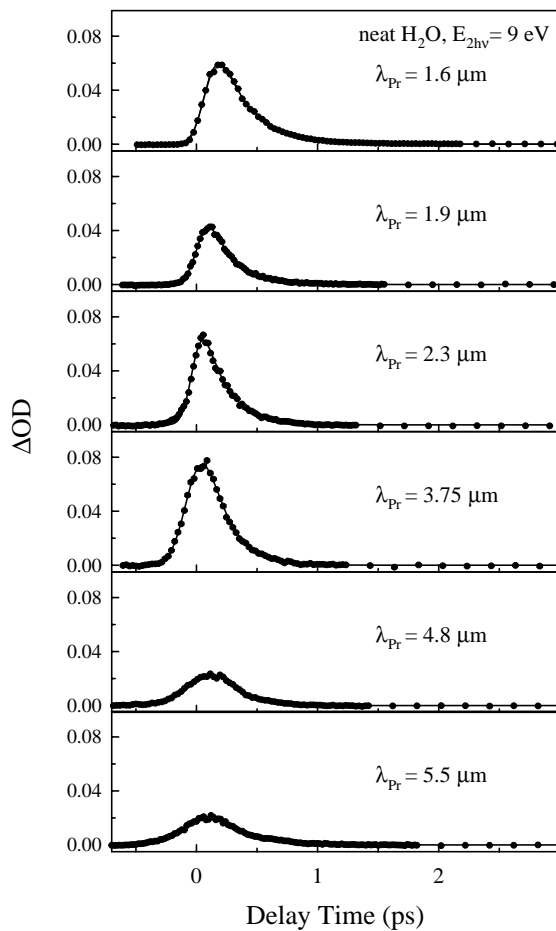


FIG. 1. Induced probe absorption of neat water after fs excitation via two photon absorption at 273 nm is demonstrated here. Signal transients in the range of 1.6 up to 5.5  $\mu\text{m}$  are shown for parallel pump and probe polarization.

effect (see below). This initial step is obviously also responsible for the observed vanishing of the induced dichroism. The subsequent relaxation proceeds with time constant  $\tau_1$  (110 fs) to a second intermediate (level 3) with absorption peak at 1.6  $\mu\text{m}$  and a lifetime  $\tau_2$  (200 fs). The following species that contributes to the transient spectrum is the already well-known wet electron (level 4). The corresponding absorption is in the NIR, only slightly redshifted to  $\approx 900$  nm in comparison to the equilibrated hydrated electron [10,11]. The lifetime of the wet electron is found again to  $\tau_{\text{hyd}} \approx 540$  fs in good agreement with earlier results [10,11]. With an efficiency of 64% long-lived solvated electrons (level 5) are generated in their ground state  $1s$  while the remaining part returns via geminate recombination to the ground state of water molecules with a time constant of  $T_{\text{GR}} \approx 2.5$  ps.

We have computed numerical solutions of rate equations describing the six-level model of Fig. 3, taking also the finite durations of the pump and probing pulses properly into account. Results of the fitting procedure are shown in Fig. 1 (calculated curves) and in Fig. 4. The respective molar extinction coefficients of intermediates (2, hollow

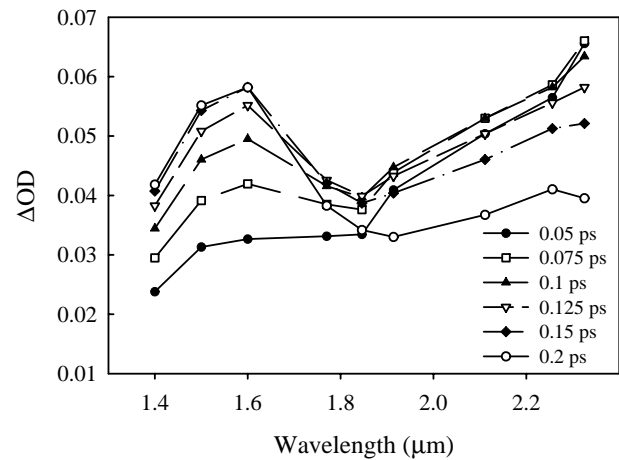


FIG. 2. Time-resolved probe absorption spectra in the wavelength range 1.4–2.35  $\mu\text{m}$  for the water sample of Fig. 1 as derived from the data partially shown there; six delay time settings from 50 fs (filled circles) to 200 fs (hollow circles). A transient isosbestic point is seen at 1.85  $\mu\text{m}$  for delay times between 75 fs (hollow squares) and 150 fs (filled diamonds).

circles) and (3, filled circles) of neat heavy water as derived from fitting the six-level scheme to the experimental data are presented in Fig. 4a (left-hand ordinate scale). Corresponding data for neat protonated water are plotted in Fig. 4b. The conventional IR absorption of the 75  $\mu\text{m}$  thick sample cell is also shown for comparison (dotted curves, right-hand ordinate scale). The latter is dominated by the strong absorption band of the hydroxylic stretching vibrations of water preventing probe absorption measurements close to the band center; some other peaks also show up, corresponding to combination tones. The absolute numbers of the left ordinate scale originate from a comparison of our probe absorption for the hydrated electron (species 5) with published values (data not shown).

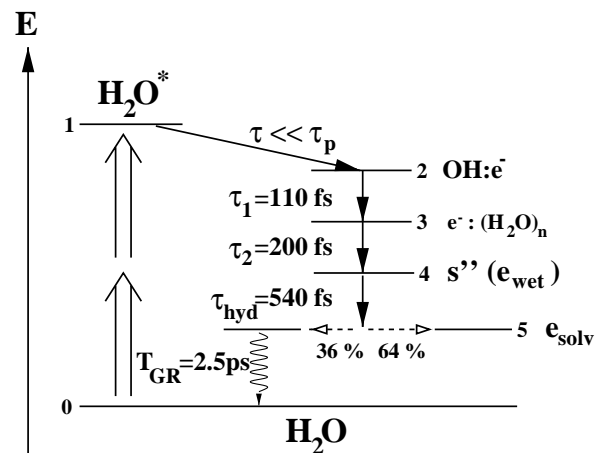


FIG. 3. Energy level scheme used to account for the measured dynamics during the generation of solvated electrons in neat water. Relaxation times are for protonated tridistilled water; for details, see text.

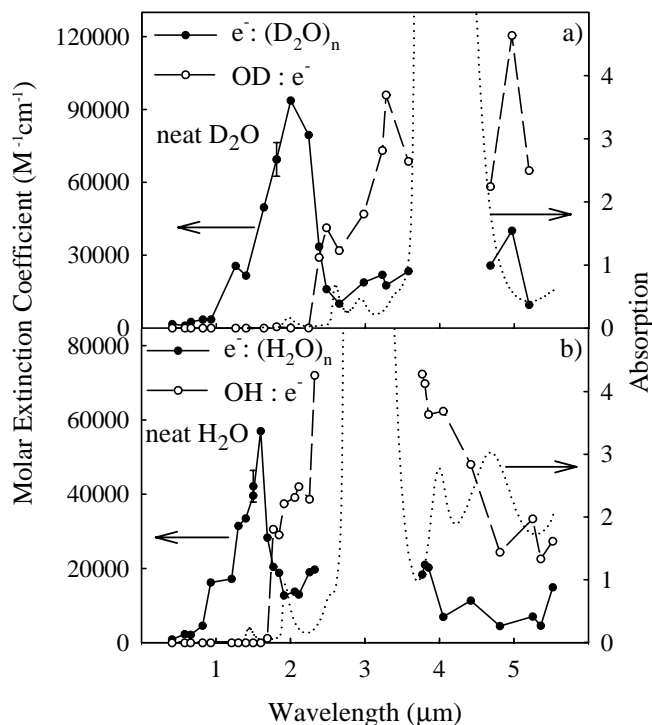


FIG. 4. Infrared molar extinction coefficient (left-hand ordinate scale, experimental points) versus wavelength of the two novel precursors (2,3) of the hydrated electron (5) in neat heavy water (a) and neat water (b). The spectra are derived from numerical fitting of the theoretical model of Fig. 3 to the experimental data. The conventional IR absorption of the sample (thickness  $75 \mu\text{m}$ ) is shown for comparison (dotted lines, right-hand ordinate scale).

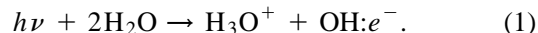
It is interesting to see that the first intermediate (2) displays a strong absorption positioned at  $\approx 2.9 \mu\text{m}$ , close to the peak absorption of the OH stretch, but notably broader (Fig. 4b, dashed line). The corresponding data for species (2) in D<sub>2</sub>O in Fig. 4a (dashed line) indicate a redshift to  $\approx 4.1 \mu\text{m}$ , close to the peak of the OD stretching band, but again notably wider than the latter. The large deuteration effect and position of the absorption feature points towards a close relationship to the OH (OD) stretching mode; it should be noted, however, that the measured absorption coefficient in Fig. 4 (left ordinate scale) exceeds that of bulk water by more than 2 orders of magnitude.

For the second intermediate (3) we find a peak absorption at  $1.6 \mu\text{m}$  (Fig. 4b, solid line) with an extended wing to longer wavelengths. For heavy water (Fig. 4a) the maximum shifts to a longer wavelength of  $\approx 2.0 \mu\text{m}$  and is spectrally broader than for the protonated case.

The lifetimes of the first two intermediates (2) and (3) are determined from our model to be  $\tau_2 = 110 \pm 40 \text{ fs}$  and  $\tau_3 = 200 \pm 40 \text{ fs}$ , respectively. The convolution of these two time constants in the subsequent relaxation steps is in accordance with the time constant for the reported buildup of the wet electron with  $\tau_{\text{tr}} = 180 \pm 50 \text{ fs}$  for  $8.8 \text{ eV}$  two photon excitation [10] and also  $180 \pm 40 \text{ fs}$  found by the Eisenthal group ( $8 \text{ eV}$ ) [11]. In contrast to

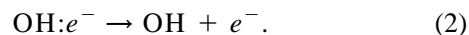
the spectral changes, the dynamics of species (2) and (3) is found to be insensitive upon deuteration:  $\tau_2$  and  $\tau_3$  are determined to be  $100 \pm 40$  and  $170 \pm 40 \text{ fs}$ , respectively, for heavy water. The results of the fitting procedure for levels (4) and (5) are already mentioned above in context with Fig. 3.

The charge separation in water at  $9 \text{ eV}$  excitation energy is below the direct Born-Oppenheimer ionization threshold [12,13]. Taking this into account, we arrive at the following interpretation of our data: Among the two reaction channels proposed in the literature for indirect photoionization [12,14], only the proton transfer mechanism starting from the excited molecule  $\text{H}_2\text{O}^*$  (level 1 in our model) appears to be consistent with our findings:



We propose here that the electronically excited  $\text{OH}^-$  considered previously for Eq. (1) has to be replaced by an OH:electron complex, for which the large IR absorption cross sections are plausible. The first intermediate (2) derived from the analysis of our data is, consequently, assigned to an OH: $e^-$  complex (OD: $e^-$  in heavy water) characterized by a strongly increased and broadened absorption of the hydroxylic stretching vibration and a lifetime of  $\approx 100 \text{ fs}$ . It is interesting to note that similar peak values to our maximum extinction coefficient of  $90\,000 (\text{Mcm})^{-1}$  of the first intermediate (2) were found for  $(\text{H}_2\text{O})_6^- \text{Ar}_n$  clusters in the gas phase [15]. The explanation there was “hydrogen bonding” of the  $e^-$  to “free” OH groups of molecules of the charged cluster [16,17]. Theoretical studies of water clusters have shown that the interaction of an OH group with an electron shifts the stretching mode frequency and enhances the absorption cross section [17,18]. An analogous phenomenon is considered here for an OH radical interacting with an electron. It is recalled that the two water molecules in Eq. (1) are embedded in the H-bridge bond network of the liquid. The hydrogen bond between the two molecules probably serves as a mediator for the proton transfer. Similarly, the oxygen of the OH: $e^-$  complex is believed to be still H bonded to the network, effecting the charge distribution of the anticipated complex. The real structure of this complex and details of the respective OH-bond length can, however, until now not be extracted from our data. This is a challenging problem to theoretical investigations which will be hopefully conducted in the near future.

The  $\text{H}_3\text{O}^+$  cation which builds up simultaneously cannot be identified from the present investigations as the maximum extinction coefficient of the OH group in water is a factor of 50 to 100 smaller in comparison to the one of the OH: $e^-$  complex. The subsequent reaction step towards the formation of hydrated electrons obviously is the electron detachment,



The generation of the OH radical in the indirect

photoionization of water was verified very recently [13]. The released electron is expected to undergo solvation phenomena. The second intermediate (3) is, consequently, interpreted as a trapped electron, but not in its final environment; the effective number of water molecules involved is suggested to be smaller than for the “wet” and fully hydrated electron (species 4 and 5 in our model, respectively). The spectral signature of species (3) is remarkably different to that of the wet electron (4) [8,11]. The interpretation is supported by results on the absorption of electrons in water clusters in the gas phase with known number  $n$  of molecules [19]. From longer wavelengths for  $n = 6$ , the peak absorption shifts with increasing cluster size to the NIR, i.e.,  $\approx 1.6 \mu\text{m}$  for  $n = 15$  molecules in the gas phase [19]. Because of the long-wavelength tail, we interpret the absorption of intermediate (3) in Fig. 4 (filled circles) as a superposition of the absorption of electrons in traps of different sizes. The assumption of preexisting traps in the liquid is consistent with the findings. In the liquid the quoted value of  $n$  responsible for the band maximum may not represent the number of nearest neighbors of the solvation shell only, but also include a contribution of more distant molecules.

The redshift and broadening of species (3) in Fig. 4a upon deuteration may be explained by a slower structural dynamics of the heavy water molecules so that the contribution of electrons in smaller traps at longer wavelengths shows up more clearly. The similarity of the absorption band of species (3) with that of the wet electron [8] and of the equilibrated solvated electron apart from a redshift suggests that intermediate (3) represents partially solvated electrons in their electronic ground state. It is recalled that the wet electron was recently identified as a fully solvated electron in a modified  $1s$  ground state due to nonequilibrium (“hot”) solvation shells. It is reasonable to assume that also the molecules forming the trap of species (3) are notably above thermal equilibrium. Correspondingly, the constant  $\tau_3 \approx 200$  fs for the transition to (4) represents the buildup time for the full layer.

The authors thank A. Thaller for computational support in numerical fitting of the data.

- 
- [1] See, for example, *Water, A Comprehensive Treatise*, edited by F. Franks (Plenum Press, New York, 1972).
  - [2] A. Migus, Y. Gauduel, J.L. Martin, and A. Antonetti, *Phys. Rev. Lett.* **58**, 1559 (1987).
  - [3] F.H. Long, H. Lu, and K. B. Eisenthal, *Phys. Rev. Lett.* **64**, 1469 (1990).
  - [4] Y. Gauduel, S. Pommeret, and A. Antonetti, *J. Phys. Chem.* **97**, 134 (1993).
  - [5] C. Silva, P.K. Walhout, K. Yokoyama, and P.F. Barbara, *Phys. Rev. Lett.* **80**, 1086 (1998).
  - [6] M.F. Emde, A. Baltuska, A. Kummrow, M.S. Pshenichnikov, and D.A. Wiersma, *Phys. Rev. Lett.* **80**, 464 (1998).
  - [7] M. Assel, R. Laenen, and A. Laubereau, *J. Phys. Chem.* **A102**, 2256–2262 (1998).
  - [8] M. Assel, R. Laenen, and A. Laubereau, *J. Chem. Phys.* **111**, 6869–6874 (1999).
  - [9] M. Assel, R. Laenen, and A. Laubereau, *Chem. Phys. Lett.* **317**, 13–22 (2000).
  - [10] A. Reuther, A. Laubereau, and D.N. Nikogosyan, *J. Phys. Chem.* **100**, 16 795 (1996).
  - [11] H. Lu, F.H. Long, and K. B. Eisenthal, *J. Opt. Soc. Am. B* **7**, 1511 (1990).
  - [12] E. Keszei and J.-P. Jay-Gerin, *Can. J. Chem.* **70**, 21 (1992).
  - [13] C.L. Thomsen, D. Madsen, S.R. Keiding, and J. Thøgersen, *J. Chem. Phys.* **110**, 3453 (1999).
  - [14] M.U. Sander, K. Luther, and J. Troe, *Ber. Bunsen-Ges. Phys. Chem.* **97**, 953 (1993).
  - [15] P. Ayotte, Ch.G. Bailey, J. Kim, and M.A. Johnson, *J. Chem. Phys.* **108**, 444 (1998).
  - [16] Ch.G. Bailey, J. Kim, and M.A. Johnson, *J. Phys. Chem.* **100**, 16 782 (1996).
  - [17] T. Tsurusawa and S. Iwata, *Chem. Phys. Lett.* **315**, 433 (1999).
  - [18] R. N. Barnett, U. Landman, and A. Nitzan, *J. Chem. Phys.* **89**, 2242 (1988).
  - [19] P. Ayotte and M.A. Johnson, *J. Chem. Phys.* **106**, 811 (1997).